npj | science of food

Article

Published in partnership with Beijing Technology and Business University & International Union of Food Science and Technology

https://doi.org/10.1038/s41538-025-00483-y

Oyster shells water extract ameliorates propylthiouracil-induced goitre in rats via PI3K/AKT/Bcl-2 pathway

Hongyi Zhang[1], Qiaoling Ma[1], Weichao Wang[1], Bin Wang[1], Jiawen Liu[1], Fu Wang[1], Yuan Hu[1], Lin Chen[1], Youping Liu[1], Qi Wang[2] ✉ & Hongping Chen[1] ✉

Oysters are recognized for flavor and health benefits, but their shells are regarded as waste, contributing to resource inefficiency. This study investigates the chemical composition and pharmacological activity of oyster shells, using a fraction partitioning approach to separate the oyster shells water extract (WE) into two fractions: WE of extra-membranous (WEE, <1000 kDa) and intra-membranous (WEI, >1000 kDa). Using UPLC-Q-Exactive MS, 231 components were identified such as organic acids, amino acids. ELISA analysis revealed that high-dose WEE significantly increased serum T3, T4, FT3, and FT4 levels while reducing TSH, and improved thyroid tissue lesions. Network pharmacology identified 291 drug-disease intersection targets enriched in the PI3K/AKT pathway. Furthermore, the RT-qPCR and WB results showed that high-dose WEE protected against propylthiouracil-induced goitre by inhibiting the PI3K/AKT/Bcl-2 pathway. This study evaluated the anti-goitre potential properties of WE and provided a theoretical basis for further development of oyster shells as a functional food source.

Oysters, saltwater bivalve molluscs inhabiting marine and brackish environments, represent a valuable marine resource with notable nutritional and medicinal benefits[1]. Globally, oysters are extensively cultivated and hold significant commercial importance. With over two millennia of cultivation history, more than 100 oyster species are farmed worldwide, including the Suminoe oyster (*Crassostrea ariakensis*), Pacific cupped oyster (*Crassostrea gigas*), Dalian Bay oyster (*Ostrea talienwhanensis*), and Hong Kong oyster (*Magallana hongkongensis*), among others[2,3]. According to statistics from the Food and Agriculture Organization of the United Nations (2018; http://www.fao.org/fishery/statistics/en)[4], global oyster production reached approximately 6.1 million tons (live weight) in 2018, yielding an estimated 4 million tons of shells, which pose considerable environmental challenges. To optimize the use of oyster resources, researchers have explored bioactive compounds from various oyster components for applications in medicine and healthcare.

Oyster meat is globally favored and consumed around the world for its tender texture, appealing taste, and rich nutritional profile. It contains various components, comprising proteins, polysaccharides, lipids, and minerals[5]. The protein content of oyster meat (on a dry weight basis) ranges from 39.1% to 53.1%[6], and it exhibits diverse biological activities. Notably, peptides derived from hydrolyzed oyster proteins demonstrate multiple bioactive properties, including antioxidant[7–9], anti-inflammatory[10,11], antibacterial[12], anticoagulant[1], anticancer[13–15], and antihypertensive[16–19] properties. These features underscore the culinary and medicinal value of oyster meat and positioning it as a focus of current research. In contrast, oyster shells, by-products of oyster processing, offer diverse applications in medicine, health foods, and ecological fields. Representing approximately 60% of the total oyster mass, oyster shells primarily consist of calcium carbonate (over 90%), supplemented a minor organic matrix (0.1 to 5%)[20,21]. This matrix protects the soft tissues and contains polysaccharides and trace inorganic elements such as zinc and selenium[22,23]. Research indicates that oyster shells possess a range of bioactive properties, including anti-osteoporotic[23,24], anti-inflammatory[25], anti-fibrotic[26], antibacterial (against Escherichia coli, lactic acid bacteria, and yeasts)[20,27,28], and antimicrobial[29,30] effects, as well as the ability to promote osteogenesis[31,32]. In China, oyster shells are recognized as a traditional Chinese medicine and are included in the *Chinese Pharmacopoeia*. Ground oyster shell powder is widely used in health foods, food additives and animal feed, with significant potential as a functional food ingredient[30,33]. Calcined oyster shell powder has gained attention for its biocompatibility and antimicrobial properties[34,35], making it a promising alternative for use as a preservative in food processing and packaging, extending shelf life and preventing foodborne illnesses. Additionally, oyster shell powder mitigates water eutrophication[36–38], regulates soil properties[39–41], and removes air pollutants. It also serves as a raw material for material synthesis[42] and construction applications[43–45]. In summary,

[1]State Key Laboratory of Southwestern Chinese Medicine Resources, Department of Pharmacy, Chengdu University of Traditional Chinese Medicine, Chengdu, China. [2]Jiangmen Institute for Drug Control, Jiangmen, China. ✉e-mail: 79657414@qq.com; chen_hongping@126.com

oyster shells possess considerable commercial, nutritional and medicinal value. Analysing their chemical composition and bioactivity is crucial for the comprehensive development and sustainable utilisation of oyster resources.

Goitre, an endocrine disorder, is a common pathological manifestation of various thyroid diseases, including autoimmune thyroiditis and nodular goitre, and primarily arises from chronic thyroid tissue hyperplasia[46]. Pathological changes in goitre are characterized by the proliferation of thyroid follicular cells, alterations in colloid cell content (accumulation or reduction), and connective tissue hyperplasia. The aetiology and pathogenesis of goitre are complex and multifactorial, with increased demand for thyroid hormones or dysregulated thyroid hormone secretion being central to its development[47,48]. In recent years, the prevalence of nodular goitre has risen, underscoring its status as a persistent global public health challenge[49]. Early clinical manifestations are often subtle and easily overlooked, resulting in delayed diagnosis and treatment. As the disease progresses, patients may develop thyroid dysfunction, which can lead to malignant transformation and pose significant threats to life[50]. Current therapeutic options for goitre include anti-thyroid medications, hormone therapy, and surgical interventions[51]. However, these approaches carry risks such as recurrence, complications, and substantial trauma[52,53], highlighting the need for safer and more effective treatments. Traditional Chinese medicine has a long-standing history of addressing goitre (thyroid diseases, including goitre)[54]. Oyster shells, a commonly used component in traditional Chinese medicine, are reputed for their ability to "soften hardness and dispel nodules", a property documented since the Song Dynasty and recognized in the *Chinese Pharmacopoeia*. Studies have demonstrated that water extracts from oyster shells exert therapeutic effects on methimazole-induced goitre in rats[55]. However, the chemical composition of these extracts remains largely uncharacterized, limiting further research into their pharmacological mechanisms. Overall, oyster shells exhibit potential anti-goitre properties, but comprehensive studies on their chemical constituents and mechanisms of action are lacking.

This study focuses on the Suminoe oyster (*Crassostrea ariakensis*) with resource-rich, and the purpose is to clarify the therapeutic effect and potential mechanism of oyster shell water extract on PTU-induced goitre in rats. Using a "fraction partitioning" strategy, the oyster shells water extract (WE) was separated into two fractions based on molecular weight: the oyster shells water extract of extra-membranous (WEE, <1000 Da) and the intramembranous (WEI, >1000 Da) fraction. The objective is to comprehensively characterize the chemical composition of the Suminoe oyster shells water extract and elucidate its mechanism of action in mitigating propylthiouracil (PTU)-induced goitre in rats. Initially, untargeted metabolomics using UPLC-Q-Exactive MS was applied to analyze the chemical constituents of WE, WEE and WEI. Animal experiments were then conducted to assess the therapeutic effects of these fractions on PTU-induced goitre in rats, with evaluations based on serum indicators of triiodothyronine (T3), thyroxine(T4), free triiodothyronine (FT3), free thyroxine (FT4), and thyroid stimulating hormone (TSH), and histopathological examination (HE staining) of thyroid tissues. Subsequently, network pharmacology was employed to identify potential bioactive components and signaling pathways involved in the anti-goitre effects. Finally, real-time quantitative reverse-transcription polymerase chain reaction (RT-qPCR) and Western blot (WB) analyses were used to investigate the expression of genes and proteins associated with the PI3K/AKT/Bcl-2 pathway in rat thyroid tissues, further confirming the mechanisms of action. Overall, this study highlighted the potential of oyster shells as a source of bioactive components with anti-goitre properties. Collectively, the findings provided valuable insights into their chemical composition and therapeutic mechanisms, offering a theoretical foundation for the medicinal application of oyster shells and promoting their comprehensive development and utilization.

Results

Preparation and characterization of the oyster shells water extract

The schematic diagram of the preparation process for the oyster shells water extracts is illustrated in Fig. 1A, with the morphologies of WEE, WE, and WEI shown in Fig. S1. The total ion chromatograms provided extensive mass spectrometric information by UPLC-Q-Exactive MS (Fig. S2). A total of 231 metabolites were identified across the three samples based on molecular weight and major fragment ions (Table S1).

These metabolites were categorized into 13 categories (Fig. 1B), including 58 organic acids and their derivatives (25.11%), 53 amino acids and their metabolites (22.94%), 34 phenolic compounds and their derivatives (14.72%), 28 fatty acyls (12.12%), 16 nucleotides and their metabolites (6.93%), 10 alcohols and amines (4.33%), 9 hormones and hormone-related compounds (3.90%), 6 heterocyclic compounds (2.60%), 6 bile acids (2.60%), 4 other species (1.73%), 3 carbohydrates and their metabolites (1.30%), 2 aldehydes, ketones, and esters (0.87%), and 2 terpenoids (0.87%).

Principal component analysis (PCA) extracted of two principal components (PC1 and PC2), accounting for 58.68% and 18.25% of the total variance, respectively. The tight clustering of the three replicate quality control (QC) samples confirmed the reliability and reproducibility of the experiment. Notably, WEI was distinctly separated from WE and WEE in the PCA plot (Fig. 1C), indicating significant differences among the three extracts. Furthermore, heatmap clustering (Fig. 1D) revealed clear distinction in metabolite content among WEI, WE, and WEE. Notably, while the metabolite species were consistent across the samples, their concentrations varied significantly (Table S1). In the comparisons between the two groups, metabolites were considered significantly different if their variable importance in projection (VIP) values exceeded 1.0 and their p-values or false discovery rates (FDR) from univariate analysis were less than 0.05. Comparative analyses revealed the following: compared to WEE, 108 metabolites were downregulated and 29 were upregulated in WEI; in contrast, 54 metabolites were upregulated and 55 were downregulated in WE. Compared to WE, 106 metabolites were downregulated and 41 were upregulated in WEI.

Oyster shells water extract improves thyroid function in PTU-induced rats

The schematic diagram of the animal experiment design is shown in Fig. 2A. The rats were gavaged with PTU solution (0.01 g/kg/d) for 2 consecutive weeks, the model group exhibited a significant increase in thyroid index and serum TSH levels, accompanied by a significant reduction in serum T3, T4, FT3, and FT4 compared to the control group. These results confirmed the successful establishment of the goitre model (Fig. 2B–G).

After 2 weeks of modeling, all treatment groups exhibited a significant reduction in body weight compared to the control group. During the treatment period, rats in the control group remained healthy, maintaining normal water and food intake, with smooth and glossy fur. In contrast, rats in the model group rats showed a slower rate of weight gain. Post-treatment, rats in the WEE-H, WE-H, and Euthyrox groups demonstrated increased body weight compared to the model group (Fig. 3A). After 4 weeks of treatment, the thyroid weights and thyroid indexes (thyroid-body weight ratio, g/kg) in all groups remained higher than those in the control group. However, thyroid indexes in the Euthyrox and WEE-H groups were significantly lower than those in the model group (Fig. 3B–C). Furthermore, serum levels of T3, T4, FT3, and FT4 were elevated, and TSH levels were reduced in all treatment groups compared to the model group. Notably, the Euthyrox and WEE-H groups exhibited significant improvements, with increased serum levels of T3, T4, FT3, and FT4 and reduced TSH (Fig. 3D–H). These results preliminarily indicate that high-dose WEE can improve thyroid function in PTU-induced rats.

Oyster shells water extract restores the pathological thyroid tissue morphology of PTU-induced rats

In this study, the thyroid tissue conditions and pathological sections of rats in each group were compared (Fig. 4A–C). In the control group, the thyroid follicles appeared normal, with a round or oval shape. The follicular cavities were filled with abundant colloid, and the follicular epithelial cells were normal, displaying a single-layer cuboidal structure that was neatly arranged around the basement membrane. In contrast, the model group exhibited

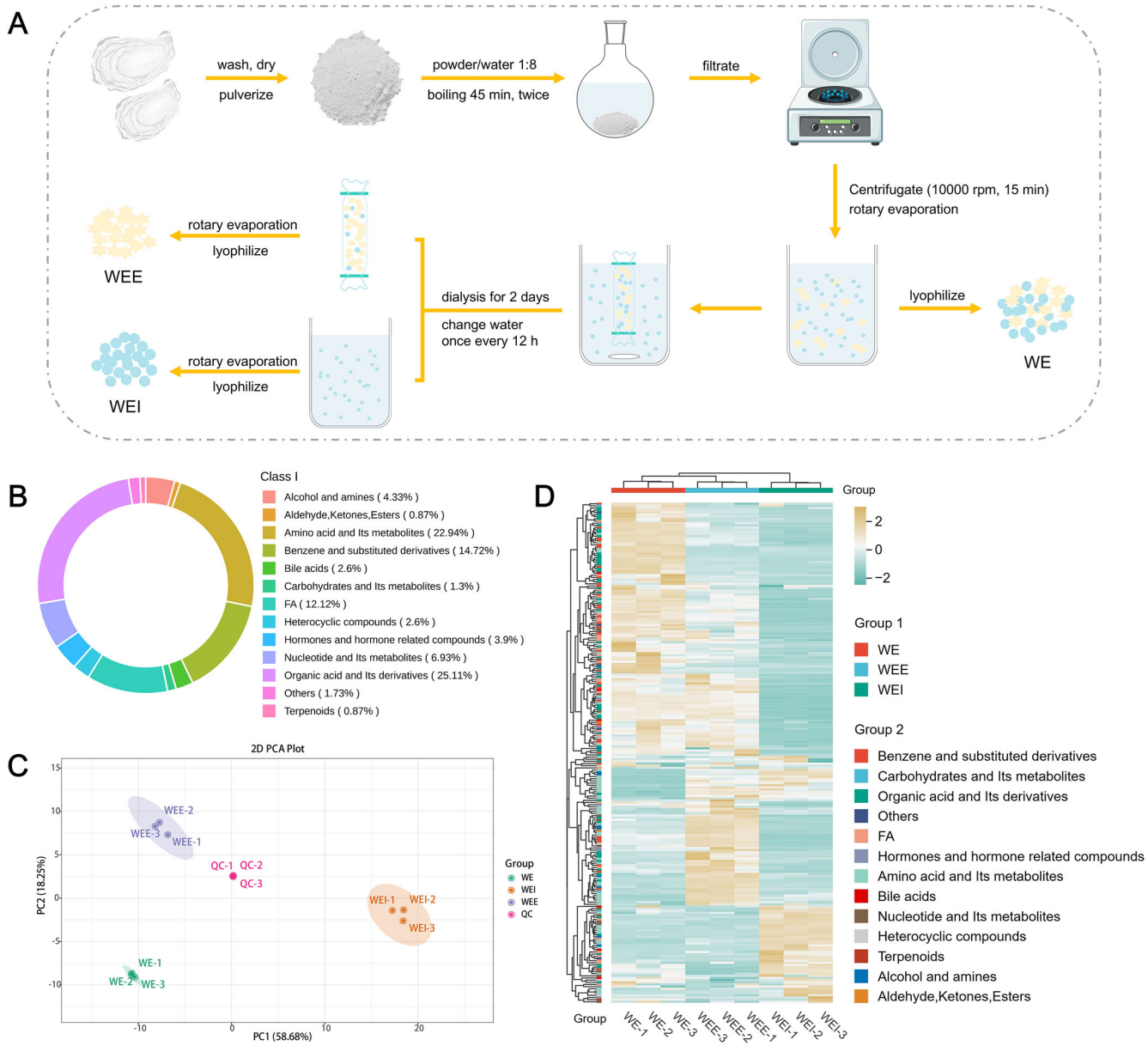

Fig. 1 | Preparation and characterization of oyster shells water extract. A The schematic diagram of the oyster water extract preparation process. The **B** metabolites classification, **C** PCA, **D** heatmap of metabolites clustering of WEE, WE, and WEI.

significant pathological alterations. The thyroid follicles showed irregular shapes and reduced follicular cavity areas. The colloid content was diminished, the number of nuclei increased and the follicular epithelial cells were hypertrophic, highly proliferative and disorganized, with blurred follicular boundaries. Following treatment, the thyroid tissue lesions in the WEE-H group of rats showed significant improvement. In this group, the majority of thyroid follicles and epithelial cells returned to normal morphology, displaying regular shapes and organized arrangements. These findings suggested that high-dose WEE improves thyroid morphology in rats with PTU-induced goitre.

Forecast analysis of network pharmacology

The biological activity of metabolites in oyster shells water extracts was assessed using the SwissTargetPrediction database, which identified 231 active components across WE, WEE and WEI, associated with 1517 related genes. Thyroid enlargement-related genes were obtained from the GeneCards database, DrugBank database, and OMIM database, resulting in 1766 disease-related genes. By overlapping the target genes of the oyster shells water extract with those associated with thyroid enlargement, 291 shared targets were identified as potential therapeutic targets for thyroid enlargement treated with oyster shells water extract (Fig. 5A). A component-target interaction network was constructed (Fig. 5B), while the PPI network analysis revealed core targets implicated in the therapeutic effects of oyster shells water extract against thyroid enlargement. And the key targets included PI3K, AKT, Bcl-2, and mTOR (Fig. 5C). Furthermore, the component-target network (Fig. 5D) highlighted key components associated with these targets, including 2-[(2-Amino-3-phenylpropanoyl) amino]-3-methylbutanoic acid, 1,11 undecanedicarboxylic acid, 2,2-dimethylglutaric acid, 9 decenoic acid, and 13 methylmyristic acid. GO analysis provided insights into the biological processes, cellular components, and molecular functions regulated by WE, WEE, and WEI (Fig. 5E). KEGG pathway analysis further identified the PI3K/AKT pathway as a potential critical mechanism through which the WE, WEE, and WEI exert anti-thyroid enlargement effects (Fig. 5F). These results will be further validated by molecular docking and molecular biology experiments.

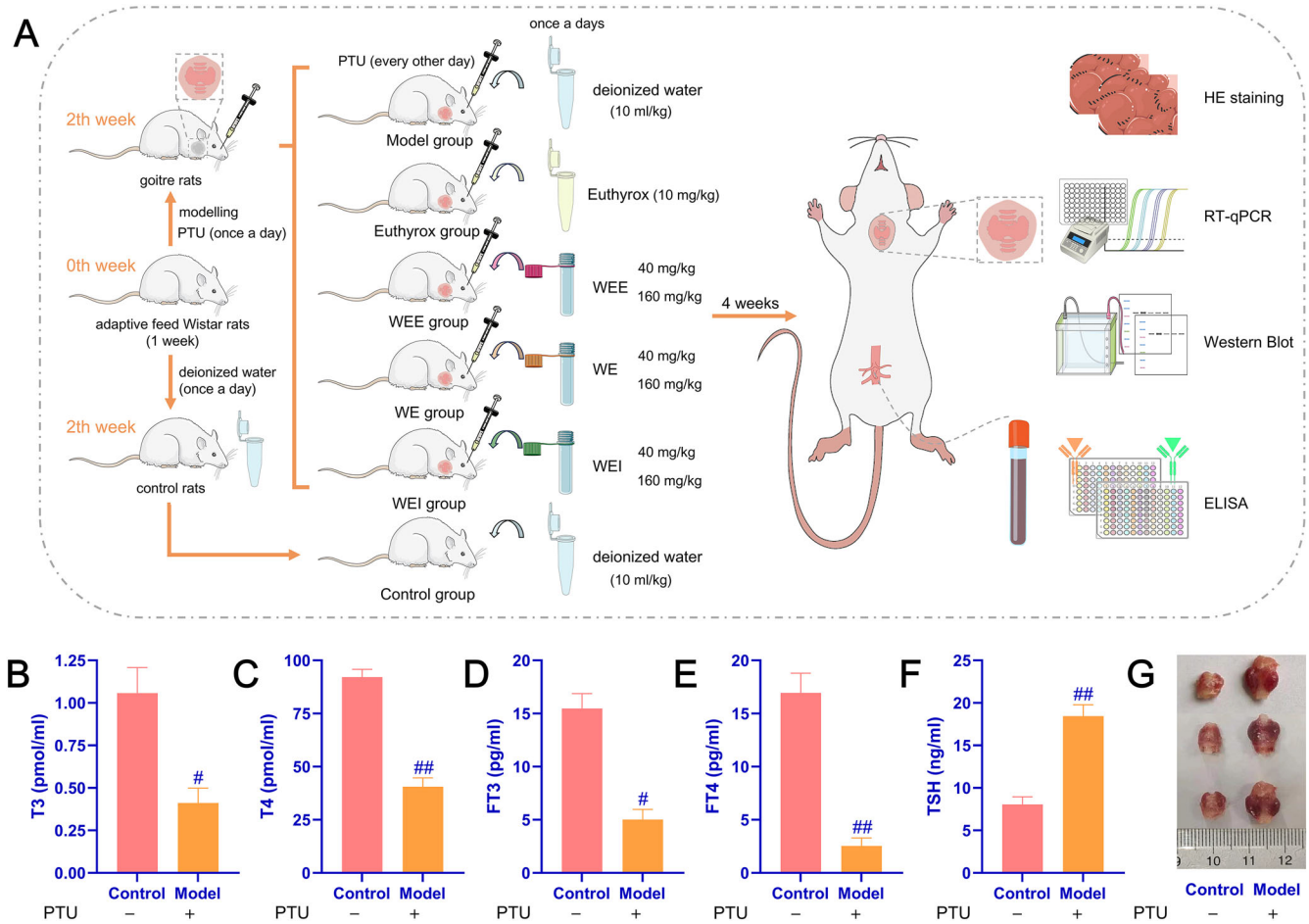

Fig. 2 | The animal experimental design, and goitre model replication. A Schematic diagram of the experimental plan of animal experiment. Serum levels of **B** T3, **C** T4, **D** FT3, **E** FT4, **F** TSH, and **G** thyroid pictures of three rats randomly chosen rats from the control and model group after PTU intragastric administration for 2 weeks ($n = 3$).

Molecular docking

Network pharmacology identified key targets of WE, WEE, and WEI in the treatment of goitre. To validate the binding affinity of the major components of oyster shells water extract with these targets, molecular docking studies were performed on five prominent compounds with the identified protein targets: PI3K, AKT, Bcl-2, and mTOR. The binding affinity between ligands and receptors was evaluated using Vina scoring (affinity in kcal/mol), where lower scores indicate more stable ligand-receptor binding. A binding affinity less than or equal to −5 kcal/mol was considered indicative of strong binding activity, and be selected as a screening standard for WE, WEE, and WEI in the treatment of goitre. For each compound-target pair, the combination with the lowest Vina score was selected for further analysis, and the binding interactions were visualized using PyMOL software. The results showed that multiple components of WEE exhibited strong binding affinities with the key targets, primarily mediated through hydrogen bonds, which contribute to the stability of these interactions (Fig. 6).

Oyster shells water extract protects PTU-induced goitre in rats through PI3K/AKT/Bcl-2 pathway

In this study, WB and RT-qPCR analysis methods were employed to validate the mechanism underlying the therapeutic effects of WE, WEI, and WEE against goitre. WB analysis was conducted to examine protein expression and phosphorylation levels of the PI3K/AKT pathway in rats thyroid tissues across different groups. Additionally, RT-qPCR analysis was used to assess the expression of key genes in the PI3K/AKT pathway in thyroid tissues.

WB analysis results are shown in Fig. 7A–H. Compared with the control group, the phosphorylation levels of PI3K and AKT proteins, as well as the expression levels of Bcl-2 protein were significantly upregulated in the thyroid tissues of the model group in rats. After therapeutic intervention with high-dose WEE, WE, or WEI, the results shown that high-dose WEE markedly inhibited the phosphorylation levels of PI3K protein and downregulated the expression levels of Bcl-2 protein; high-dose WEE and high-dose WE significantly inhibited the phosphorylation levels of AKT protein. These findings suggested that high-dose WEE effectively protected PTU-induced goitre in rats by inhibiting PI3K/AKT pathway phosphorylation and downregulating the expression levels of Bcl-2 protein.

RT-qPCR analysis results are shown in Fig. 7I–L. The results showed that the mRNA expression levels of PI3K, AKT, Bcl-2, and mTOR were significantly upregulated in the thyroid tissues of the model group in rats compared with the control group. Following treatment with high-dose WEE, WE, or WEI, the results shown that the positive drug, high-dose WEE, and high-dose WE notably downregulated the mRNA expression levels of PI3K, AKT, Bcl-2, and mTOR in the thyroid tissues of the rats. These findings confirmed that high-dose WEE can achieve an anti-goitre effect in PTU-induced rats by inhibiting the expression of related genes in the PI3K/AKT/Bcl-2 pathway.

Discussion

Previous studies have primarily focused on the macromolecular protein fraction of oyster shells water extract, neglecting small molecular metabolites. For instance, the research conducted by Feng[23,24] involved water extraction of oyster shells, followed by dialysis separation. However, only the components within the dialysis bag were collected for further experiments, while those outside the bag were disregarded. This approach limits a comprehensive evaluation and analysis of the chemical constituents and pharmacological

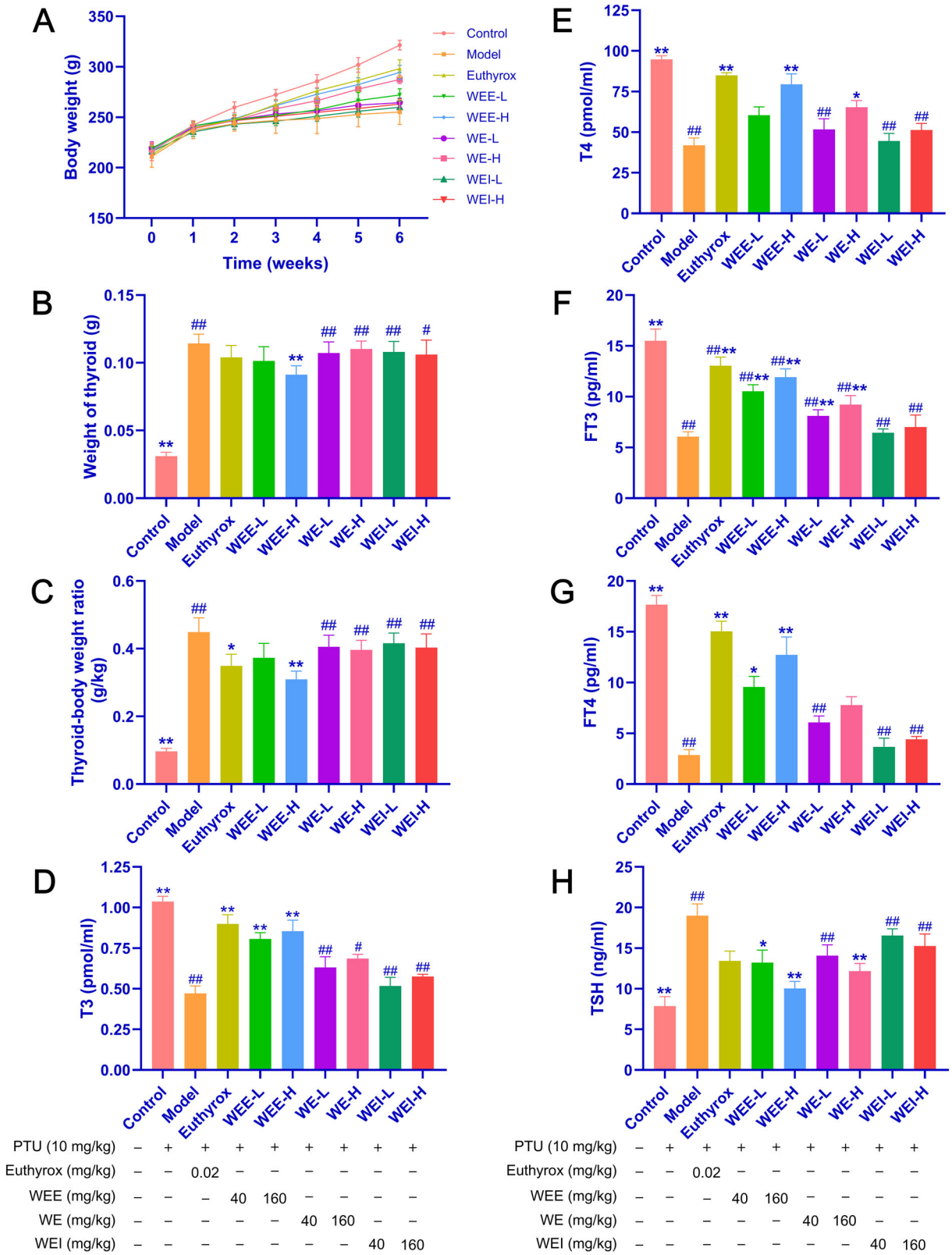

Fig. 3 | The effects of WEE, WE, and WEI on body weight, thyroid index, and serum levels of rats in each group ($n = 8$). The **A** body weight, **B** thyroid weight, **C** thyroid index, and the serum levels of **D** T3, **E** T4, **F** FT3, **G** FT4, **H** TSH of rats in each group.

basis of oyster shells water extract. In this study, we collected components from both inside and outside the dialysis bag and conducted compositional analysis and pharmacodynamic evaluation to comprehensively elucidate the pharmacological basis underlying its anti-goitre effects. And to comprehensively analyze the metabolite profiles of the extracts and elucidate the pharmacological basis underlying their anti-goitre efficacy, a novel untargeted metabolomics approach based on UPLC-Q-Exactive MS was applied for the first time to investigate the metabolites of WEE, WE, and WEI. The results shown that the oyster shells water extract mainly contains organic acids, amino acids, fatty acyls, nucleotides compounds.

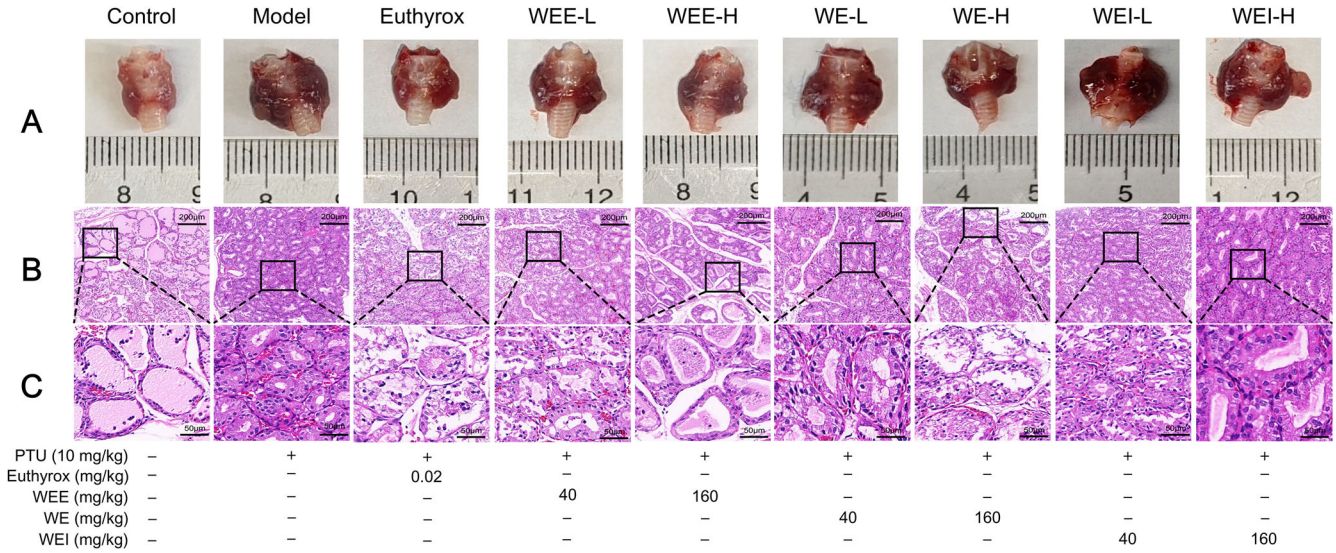

Fig. 4 | The effects of WEE, WE, and WEI on the thyroid condition and thyroid pathological state in thyroid tissue of rats in each group. A Representative images of the thyroid conditions of rats in each group; **B** HE staining (Scale bar = 200 μm); **C** HE staining (Scale bar = 50 μm).

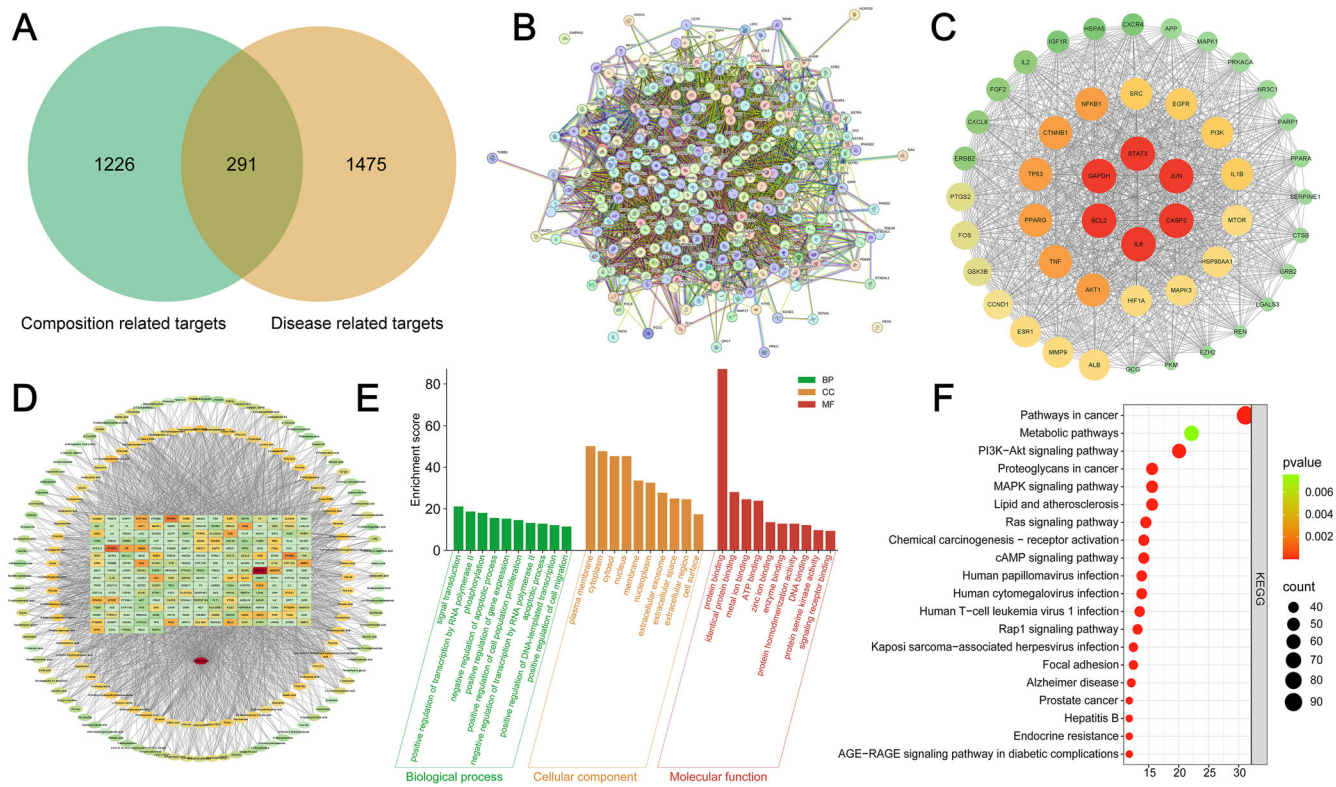

Fig. 5 | Results of network pharmacology and functional analysis. A Venn diagram of oyster shells water extract component-related targets and goitre-related targets. **B** Core potential therapeutic target PPI interaction network. **C** Network of the metabolites and the overlapping goitre-relate targets. **D** Oyster shells water extract -metabolites-target interaction network. **E** The GO analysis of potential targets. **F** The KEGG analysis of potential targets.

The occurrence and development of goitre is closely associated with abnormal thyroid hormone levels. Insufficient levels of thyroid hormones (T3, T4, FT3, and FT4) lead to increased secretion of TSH by the pituitary gland to stimulate thyroid activity. Elevated TSH levels can induce thyroid tissue hyperplasia, alter thyroid morphology and ultimately result in goitre[56]. In this study, to evaluate the efficacy of WE, WEE, and WEI on PTU-induced in rats, ELSA was employed to quantify the serum levels of T3, T4, FT3, FT4, and TSH. The results shown that Euthyrox and high-dose WEE were able to cause an increase in T3, T4, FT3, and FT4 levels, while THS levels exhibited a decrease significantly in the serum of goitre rats. Histopathological analysis provides critical insights into cellular and tissue structures, enabling the assessment of overall morphology and pathological changes. Hematoxylin and eosin (HE) staining is a widely used method in pathology for identifying lesions and evaluating the morphological features and distribution of tissue cells. These findings align with previously reported pathological changes associated with goitre[57,58]. This study only evaluated the therapeutic effects of oyster shells water extract on goiter in PUT-induced rats by using thyroid index, serum levels of T3, T4, FT3, FT4, and

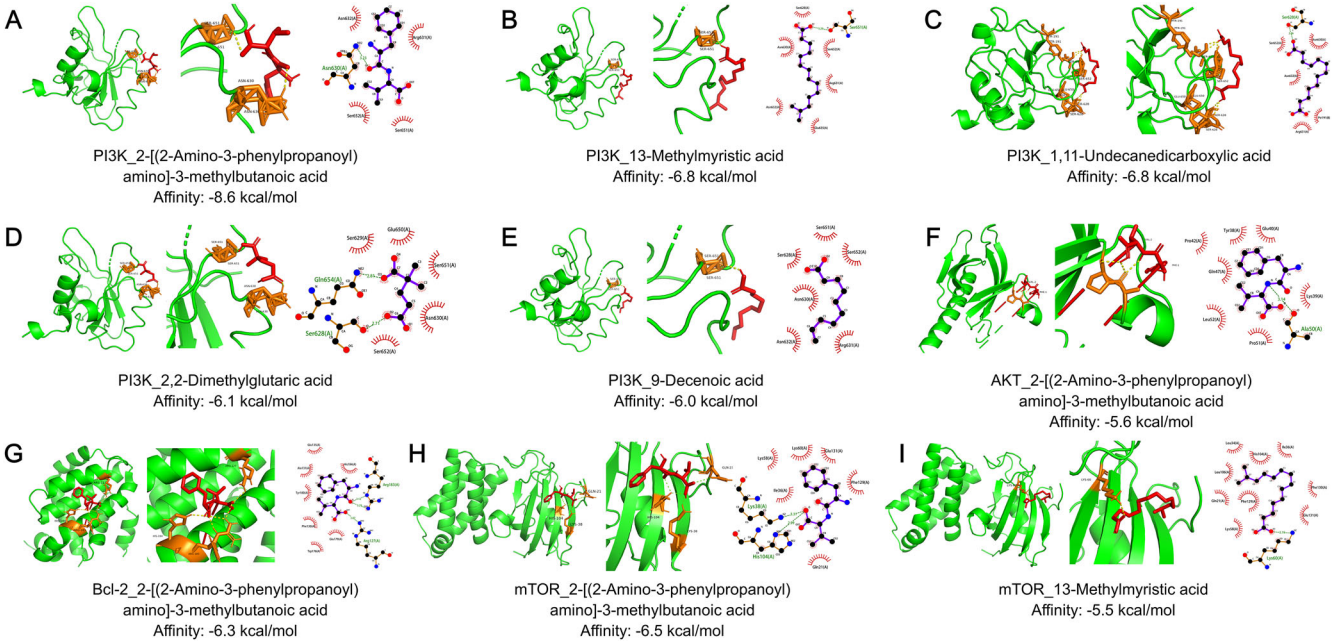

Fig. 6 | Molecular docking of the five highest-scoring compounds to the goitre-related protein targets. Molecular docking scores and sites of **A** 2-[(2-Amino-3-phenylpropanoyl) amino]-3-methylbutanoic acid with PI3K, **B** 13-Methylmyristic acid with PI3K, **C** 1,11-Undecanedicarboxylic acid with PI3K, **D** 2,2-Dimethylglutaric acid with PI3K, **E** 9-Decenoic acid with PI3K, **F** 2-[(2-Amino-3-phenylpropanoyl) amino]-3-methylbutanoic acid with AKT, **G** 2-[(2-Amino-3-phenylpropanoyl) amino]-3-methylbutanoic acid with Bcl-2, **H** 2-[(2-Amino-3-phenylpropanoyl) amino]-3-methylbutanoic acid with mTOR, **I** 13-Methylmyristic acid with mTOR.

TSH, as well as thyroid tissue morphology as indicators. However, it did not assess the related indicators of thyroid hormone synthesis and transport, which cannot fully reflect the therapeutic efficacy of the drug.

In this study, three main potential target genes PI3K, AKT, and Bcl-2 of WE for goitre therapy, were screened out by network pharmacology and molecular docking. The PI3K/AKT pathway is a critical cellular signaling cascade that plays a significant role in regulating various biological processes, including cell proliferation, autophagy, apoptosis, invasion, and migration[59,60]. Class I PI3K, a central component, catalyzes the conversion of PI(4,5)P2 to PI(3,4,5)P3, and its activation depends on receptor tyrosine kinases (Class IA) or G protein-coupled receptors (Class IB). AKT, an evolutionarily conserved serine/threonine protein kinase, is a major downstream effector of PI3K. Upon activation, AKT phosphorylates key substrates, including glycogen synthase kinase 3β (GSK-3β), preventing cyclin D1 degradation and promoting the G1 to S phase cell cycle transition, thereby accelerating cell proliferation. Additionally, the PI3K/AKT pathway can inhibit apoptosis through phosphorylation of Bcl-2-associated death promoters and activation of Bcl-2, while regulating autophagy by forming complexes with PIP3 and phosphorylating PDK1. Activation of this pathway also suppresses caspase-3 expression, reducing apoptotic activity and enhancing cell migration. Overall, the PI3K/AKT pathway influences downstream signaling molecules and cellular responses, regulating proliferation, autophagy, apoptosis and invasion, which are critical in disease progression[61–64]. The expression of several proteins involved in the PI3K/AKT pathway is depicted in Fig. 8.

Previous research has demonstrated that aberrant activation of the PI3K/AKT pathway contributes to resistance to apoptosis, accelerated proliferation and abnormal differentiation, making it a pivotal factor in thyroid disease development[56–58,65,66]. It is suggested that inhibiting the hyperactivation of the PI3K/AKT pathway can effectively prevent goitre. Based on the combined analysis results from metabolomics and network pharmacology, it was highlighted that PI3K, AKT, and Bcl-2 proteins play crucial roles on the PI3K/AKT pathway in the process of goitre. Our data elucidated that oyster shell water extract played a protective role in the goitre model rats via downregulating the PI3K/AKT/Bcl-2 pathway. However, the key components predicted to have lower binding affinity with core targets in this study have not further validated. Additionally, this study only validated the PI3K/AKT/Bcl-2 pathway, and it is necessary to consider the interaction between this pathway and other signaling pathways.

Summary, this study employed an integrative approach, combining untargeted metabolomics to identify bioactive components, network pharmacology to predict therapeutic targets, animal experiments to evaluate anti-goitre effects and molecular biology techniques to elucidate underlying mechanisms. The results demonstrated that the high-dose WEE effectively improves thyroid function of PTU-induced goitre in rats by inhibiting the activation of the PI3K/AKT/Bcl-2 pathway. These findings that provided a theoretical basis for further development of oyster shells as a functional food source, and offered insights into the utilization of oyster shell resources and the treatment of goitre.

Methods

Preparation of oyster shells water extract

The preparation and separation process of the oyster shells water extract is detailed as follows. Oyster shells were procured from a local market (Guangdong, China), thoroughly cleaned to remove surface contaminants, dried and pulverized into a fine powder. The powdered oyster shells were mixed with deionized water at a 1:8 (w/w) ratio and soaked for 12 h, followed by boiling for 45 min. This extraction process was repeated twice. The resulting filtrates were centrifuged at 10,000 rpm for 15 min and the supernatants were collected. The pooled extract was concentrated using rotary evaporation and then lyophilized to obtain oyster shells water extract (WE). The WE were subsequently fractionated using dialysis bags over two days (1000 Da, Solarbio Science & Technology Co., Ltd, Beijing, China). The intra-membranous and extra-membranous fractions were collected separately and lyophilized to obtain oyster shells water extract of extra-membranous (WEE, <1000 Da) and intra-membranous (WEI, >1000 Da).

Identification of compounds in oyster shells water extract using UPLC-Q-Exactive MS

20 mg of WE, WEE, and WEI samples were respectively mixed with 400 μL of pure water internal standards extraction solution, and vortexed for 30 s.

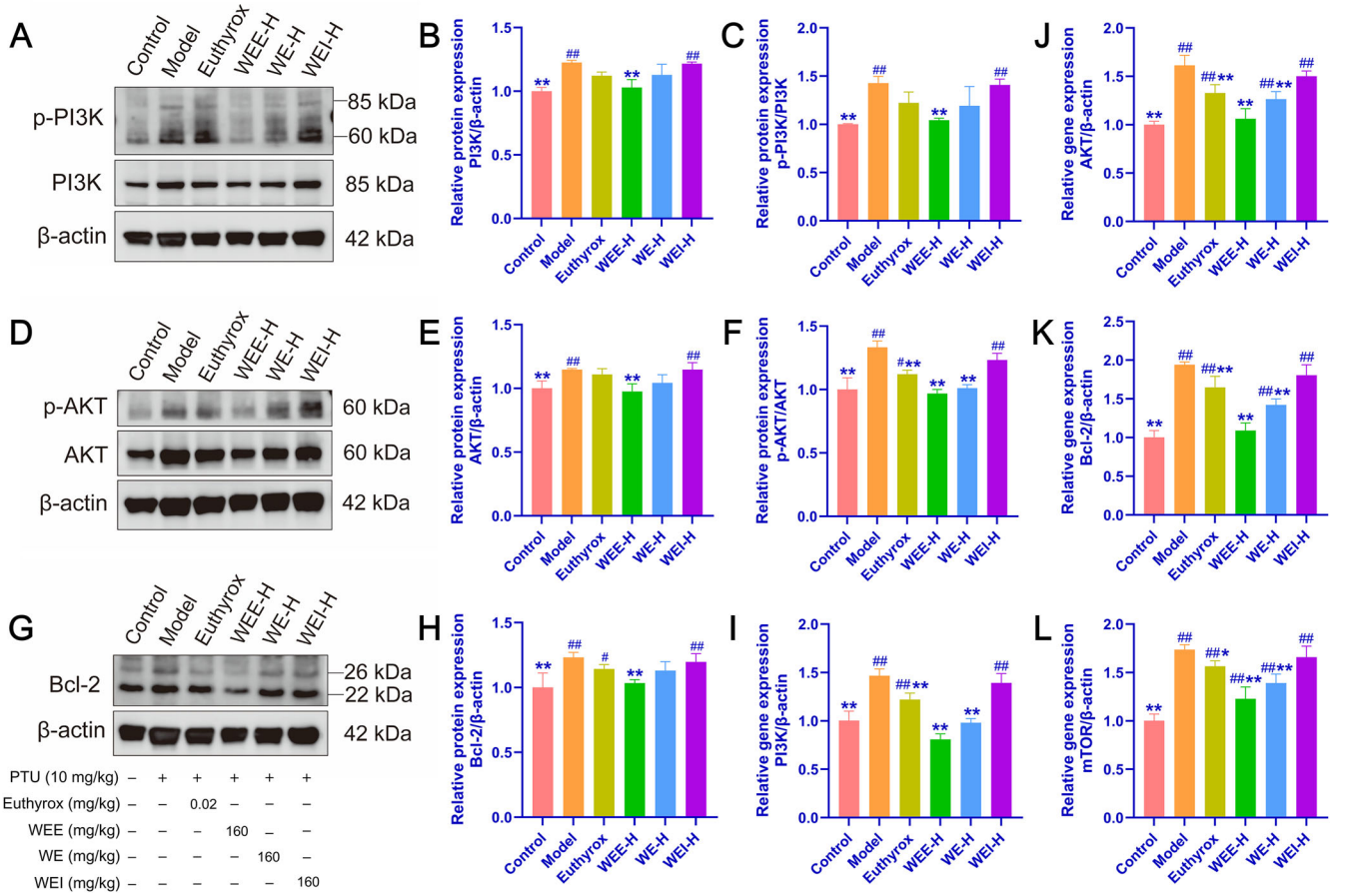

Fig. 7 | The effects of WEE, WE, and WEI on the expression levels of proteins and genes in the PI3K/AKT/Bcl-2 pathway in the thyroid tissues of goitre rats in each group. The WB analysis of **A** PI3K and p-PI3K, **D** AKT and p-AKT, **G** Bcl-2 protein levels, and the semi-quantitative analysis of **B** PI3K/β-actin, **C** p-PI3K/PI3K, **E** AKT/β-actin, **F** p-AKT/AKT, and **H** Bcl-2/β-actin ($n = 4$). The RT-qPCR analysis of (**I**) PI3K, **J** AKT, **K** Bcl-2, and (**L**) mTOR mRNA levels ($n = 6$).

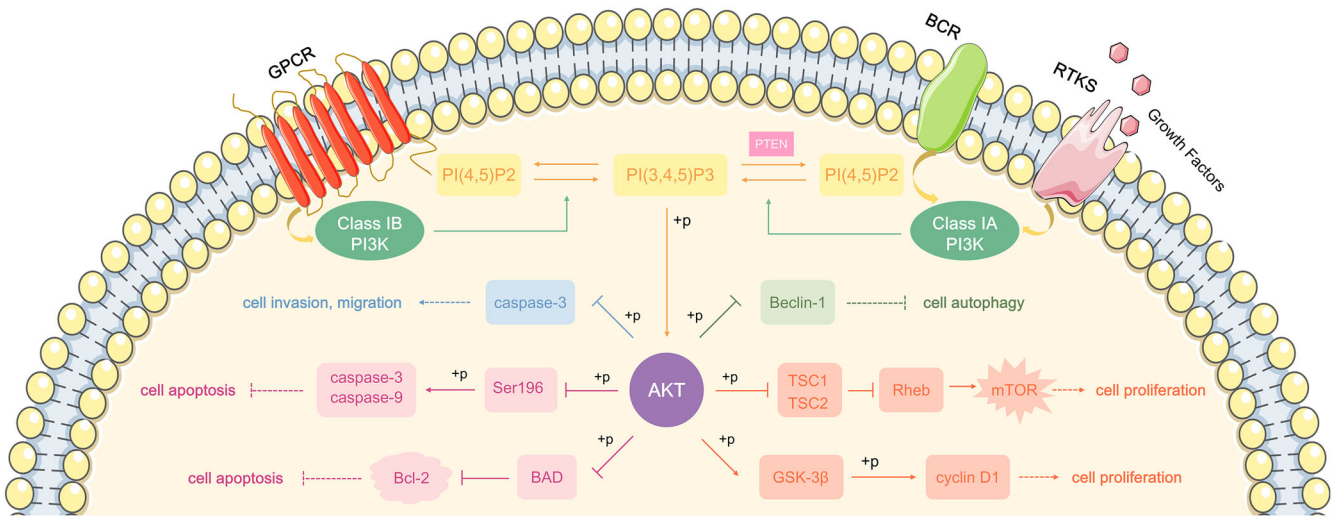

Fig. 8 | The expression of relevant proteins in the PI3K/AKT pathway (┤ represents inhibition, → represents promotion).

The samples were homogenized at 35 Hz for 3 min, and then sonicated in an ice bath for 10 min. After removing the samples, they were vortexed for 1 min, and then incubated for 30 min at −20 °C, followed by centrifugation at 12,000 rpm for 10 min at 4 °C. The supernatant was transferred to fresh injection vials for subsequent analysis. The quality control (QC) samples were prepared by mixing equal volumes of the supernatants.

The metabolite analysis was conducted using a Vanquish UPLC system (Thermo Fisher Scientific, Massachusetts, USA) with a Waters ACQUITY Premier HSS T3 Column (1.8 μm, 2.1 mm × 100 mm) coupled to an Q Exactive HF-X (Thermo Fisher Scientific, Massachusetts, USA) mass spectrometer. The detailed methods of HPLC and MS conditions shown as follows:

UPLC Conditions: One aliquot was analyzed using positive ion conditions and was eluted using 0.1% formic acid (chromatographic purity, Shanghai Aladdin Biochemical Technology Co., Ltd, Shanghai, China) in water (A) and 0.1% formic acid in acetonitrile (chromatographic purity, Merck, Darmstadt, Germany) (B) in the following gradient: 0–2 min, 5% B–20% B; 2–5 min, 20% B–60% B; 5–6 min, 60% B–99% B; 6–7.5 min, 99% B; 7.5–7.6 min, 99% B–5% B; 7.6–10 min, 5% B. The column temperature was set at 40 °C, and the flow rate was set at 0.4 mL/min with a 4 μL injection volume. Another aliquot was using negative ion conditions and was the same as the elution gradient of positive mode.

MS Conditions: All the methods alternated between full scan MS and data dependent MSn scans using dynamic exclusion. MS analyses were carried out using electrospray ionization in the positive ion mode and negative ion mode using full scan analysis over m/z 75–1000 at 35,000 resolutions. Additional MS settings are: ion spray voltage, 3.5 kV or 3.2 kV in positive or negative modes, respectively; Sheath gas (Arb), 30; Aux gas, 5; Ion transfer tube temperature, 320 °C; Vaporizer temperature, 300 °C; Collision energy, 30, 40, 50 V; Signal Intensity Threshold, 1*e6 cps; Top N vs Top speed, 10; Exclusion duration, 3 s.

Experimental animals and design

Seventy-eight SPF male Wistar rats (Certificate No. of SCXK (Jing)2024-0001), aged 6 weeks 180–220 g, were purchased from Spearfish Biotechnology Co., Ltd (Beijing, China). All rats were raised on regular rodent chow diet and sterilized deionized water. The rats were maintained under SPF conditions in an environment with a constant temperature of 22 ± 2 °C, relative humidity of 50 ± 10%, and a 12 h light/dark cycle. All animal experimental procedure in this study were reviewed and approved by the Medical and Laboratory Animal Ethics Committee of Chengdu University of Traditional Chinese Medicine (ethical approve number: 2024019).

After 1 week of adaptive feeding, the rats were randomly divided into a control group (n = 11) and a model group ($n = 67$). Except for the control group, all rats were administered a PTU (Shanghai Zhaohui Pharmaceutical Co., Ltd., Shanghai, China) solution (0.01 g/kg/d) via oral gavage for 2 consecutive weeks to establish a goitre model[57,58]. On the 15th day, three rats from both control group and model group were randomly selected and euthanized by intraperitoneal injection of pentobarbital sodium (150 mg/kg). Biochemical analysis showed significantly decreased serum levels of T3, T4, FT3, and FT4, along with elevated TSH levels in the model group, confirming successful modelling. Following the confirmation of successful modelling, 64 rats were randomly assigned into 8 groups, comprising the model group (Model), Euthyrox group (Euthyrox), low dose (WEE-L) and high dose (WEE-H) of WEE group, low dose (WE-L) and high dose (WE-H) of WE group, low dose (WEI-L) and high dose (WEI-H) of WEI group, with 8 rats in each group.

Once the model was successful, each group was given with the corresponding treatment measures for a duration of 4 weeks: the control group (deionized water, 10 mL/kg/d), the model group (PTU, 0.01 g/kg/d), the Euthyrox group (Euthyrox, 0.02 mg/kg/d, Merk Pharmaceutical, Darmstadt, Germany), WEE-L group (WEE, 40 mg/kg/d), WEE-H group (WEE, 160 mg/kg/d), WE-L group (WE, 40 mg/kg/d), WEI-L groups (WEI, 40 mg/kg/d), and WEI-H (WEI, 160 mg/kg/d), respectively. Based on the clinical dosage of oyster shells used in adult, the yield of the extract, and the allometric dose conversion between rats and human, WE-L was given at 1× the clinical dosage, while WE-H received 4× the clinical dosage. The high and low doses of WEE and WEI correspond to the same dosages as WE. In addition, except for the control and model groups, PTU was still given to the remains at the dose of 0.01 g/kg/d every other day during the 4 week treatment period to stabilize the goitre model. During the experimental period, the rats were given free access to food and water, and their body weight were measured and recorded once a week, while observing their behavioral status. After the final administration, all rats were fasted for 24 h with free access to water, then they were euthanized by intraperitoneal injection of pentobarbital sodium (150 mg/kg), and the blood samples were collected from the abdominal aorta. Following the blood collection, the thyroid tissue was promptly excised from both sides of the trachea, weighed, and the thyroid index was calculated. One side of the thyroid tissue was rapidly fixed in 4% paraformaldehyde solution for pathological analysis, while the other side was frozen in liquid nitrogen and stored at −80 °C for further analysis.

Biochemical analysis

After allowing the blood samples to stand at room temperature for 1 h, they were centrifuged at 1000 × g for 20 min at 4 °C, and the upper serum layer was obtained. The serum levels of FT3, FT4, and TSH were measured according to the instructions of the enzyme-linked immunosorbent assay (ELISA) kits (Elabscience Biotechnology Co., Ltd, Wuhan, China). And the T3 and T4 contents were detected using the ELISA kits (Shanghai Yuanye Biotechnology Co., Ltd, Shanghai, China) following the instructions. A comparative analysis of thyroid function among the different groups of rats was performed.

Histopathological examination staining of tissues

The fixed thyroid tissues from rats of each group were embedded in paraffin and sectioned (5 μm). The sections were stained with hematoxylin and eosin (Wuhan Servicebio Biotechnology Co., Ltd, Wuhan, China), and then dehydrated and mounted for imaging. Images were captured using an upright microscope to observe morphological changes in the tissue samples.

Network pharmacological analysis

The network pharmacology methods were employed to preliminarily predict the mechanisms of action of WE, WEE, and WEI in the treatment of goitre in rats. Based on the analysis results from UPLC-Q-Exactive MS, and in conjunction with the TCMSP database (https://old.tcmsp-e.com/tcmsp.php), potential bioactive components in WE, WEE and WEI were screened. A compound was considered to possess bioactivity if it met any of the following three criteria: a. the oral bioavailability of the compound is greater than or equal to 30%, and the drug-likeness is greater than or equal to 0.18 in the TCMSP database; b. the Molinspiration website tool (https://molinspiration.com/) predicts that the compound adheres to at least five of the calculated property guidelines or demonstrates predicted activity; c. the bioactivity of the reported compound has been demonstrated in previously published literature.

The structures and SMILES codes of these components were obtained from the PubChem database (https://pubchem.ncbi.nlm.nih.gov/). The selected bioactive compounds were then subjected to human target prediction using the SwissTargetPrediction database (http://www.swisstargetprediction.ch/) to identify potential active targets. To further screen therapeutic targets associated with goitre, we used "goitre" as a keyword to collect related targets from the GeneCards database (https://www.genecards.org/), DrugBank database (https://go.drugbank.com/), and OMIM database (https://www.omim.org/). Using the Venn 2.1 online tool (http://www.liuxiaoyuyuan.cn/), we generated a diagram of the drug-disease intersection targets to identify common targets. The STRING database (https://cn.string-db.org/) was employed to predict the protein-protein interaction (PPI) network. Cytoscape software was utilized to construct a "disease-drug-component-target" network. Additionally, we conducted gene ontology (GO) enrichment analysis and Kyoto encyclopedia of genes and genomes (KEGG) pathway analysis using the DAVID database (https://david.ncifcrf.gov/) and the METASCAPE database (https://metascape.org/gp/#/main/step1), creating visual representations of functional enrichment analysis and bubble plots for enriched pathways.

Molecular docking simulation

Based on the results from the construction of the "drug-component-target-pathway" network model, core compounds were selected as ligands for molecular docking with proteins, sorted by degree. First, the core components were downloaded in MOL2 format from the TCMSP database and converted to pdb format using Open Babel 3.1.1 software. Subsequently, the protein crystal structures of the core targets were obtained from the PDB database

(http://www.rcsb.org). Using PyMOL software, water molecules were removed, original ligands were cleared, and the structures were saved in pdb format. Next, AutoDock Tools software was employed to adjust the charges and select torsion bonds for the core components, while hydrogen atoms were added to the core targets. The structures were then imported into AutoDock Vina software in pdbqt format for molecular docking, providing evidential support for the therapeutic effects of WE, WEE, and WEI on thyroid goitre. Finally, the molecular docking results were visualized using PyMOL software, and the docking sites were predicted using LigPlus software.

Western blot analysis

The thyroid tissues thoroughly ground and homogenized in pre-cooled radio-immunoprecipitation assay (RIPA) lysis buffer (Epizyme Biotechnology Co., Ltd, Shanghai, China) and protease/phosphatase inhibitor cocktail (Beyotime Biotechnology Co., Ltd, Chengdu, China), and the centrifuged to obtain tissue proteins, and then the protein samples were heated at 100 °C for 10 min. Subsequently, the samples underwent separation via gel electrophoresis (Epizyme Biotechnology Co., Ltd, Shanghai, China), and transferred onto a polyvinylidene difluoride (PVDF) membrane, then incubated with antibodies against PI3K, p-PI3K, AKT, p-AKT, Bcl-2 (1:1000, Cell Signaling Technology, Massachusetts, USA), and β-actin (1:1000, Beyotime Biotechnology Co., Ltd, Chengdu, China) overnight at 4 °C, followed incubated with secondary antibody (1:1000, Beyotime Biotechnology Co., Ltd, Chengdu, China) for 1 h at room temperature. Finally, protein bands were captured using the eBlot Touch Imager chemiluminescent imaging system (e-Blot Life Science Co., Ltd, Shanghai, China), and semi-quantitated using Image J software.

RT-qPCR analysis

According to the specifications of the RNAprep FastPure Tissue kits (Tsingke Biotechnology Co., Ltd, Beijing, China), RNA was extracted from thyroid tissue, and then the cDNA was synthesized using reverse transcription kits. The cDNA mixed with 1.0 × EasyQ SYBR qPCR Mix (Low ROX Premixed) (Tsingke Biotechnology Co., Ltd, Beijing, China) and corresponding specific primers, then the mRNA expression of PI3K, AKT, Bcl-2, mTOR, and β-actin were detected by the Bio-Rad CFX96 Connect™ real-time PCR detection system (Bio-Rad, USA). The expression level of target gene relative was calculated using the $2^{-\Delta\Delta ct}$ method. The corresponding specific primers were used as follows:

PI3K For: GCCTCTAATCTTCTCCCTCTCCTTC
PI3K Rev: CTTGCCTCCATTCACCACCTCT
AKT For: TCACCCAGTGACAACTCAG
AKT Rev: GATCACCTTCCCAAAGGTGC
Bcl-2 For: CACGGTGGTGGAGGAACTCT
Bcl-2 Rev: TCCACAGAGCGATGTTGTCC
mTOR For: GTGTGGCAAGAGCGGCAGAC
mTOR Rev: TGTTGGCAGAGGATGGTCAAGTTG
β-actin For: CCTCTATGCCAACACAGT
β-actin Rev: AGCCACCAATCCACACAG

Statistical analysis

Statistical analyses were performed using GraphPad Prism 10.0 software and SPSS 27.0 software. Each experiment included 3–8 replicates, and data were presented as mean ± standard deviation (SD). Differences between groups were assessed using one-way analysis of variance (ANOVA) or T-tests. A significance level set up $p < 0.05$ was considered statistically significant ($^{\#}p < 0.05$, $^{\#\#}p < 0.01$ compared with control group; $^{*}p < 0.05$, $^{**}p < 0.01$ compared with model group).

Data availability

All data generated or analysed during this study are included in this published article and its supplementary information files.

Received: 2 March 2025; Accepted: 8 June 2025;
Published online: 16 June 2025

References

1. Cheng, S. et al. A novel heptapeptide derived from Crassostrea gigas shows anticoagulant activity by targeting for thrombin active domain. *Food Chem.* **334**, 127507 (2021).
2. Botta, R., Asche, F., Borsum, J. S. & Camp, E. V. A review of global oyster aquaculture production and consumption. *Mar. Policy* **117**, 103952 (2020).
3. Zhang, G., Li, L. & Que, H. An evolution of oyster mariculture industry in China: new knowledge, variety and product. *Oceanol. Limnol. Sin.* **51**, 740–749 (2020).
4. FAO. https://www.fao.org/fishery/en/statistics/en (2018).
5. Liu, L. et al. Metabolomics investigation on the volatile and non-volatile composition in enzymatic hydrolysates of Pacific oyster (*Crassostrea gigas*). *Food Chem. X* **17**, 100569 (2023).
6. Linehan, L. G., O'Connor, T. P. & Burnell, G. Seasonal variation in the chemical composition and fatty acid profile of Pacific oysters (*Crassostrea gigas*). *Food Chem.* **64**, 211–214 (1999).
7. Zhang, Z. et al. Alcalase-hydrolyzed oyster (*Crassostrea rivularis*) meat enhances antioxidant and aphrodisiac activities in normal male mice. *Food Res. Int.* **120**, 178–187 (2019).
8. Papachristoforou, E., Lambadiari, V., Maratou, E. & Makrilakis, K. Association of glycemic indices (hyperglycemia, glucose variability, and hypoglycemia) with oxidative stress and diabetic complications. *J. Diab. Res.* **2020**, 7489795 (2020).
9. Qian, B., Zhao, X., Yang, Y. & Tian, C. Antioxidant and anti-inflammatory peptide fraction from oyster soft tissue by enzymatic hydrolysis. *Food Sci. Nutr.* **8**, 3947–3956 (2020).
10. Xie, C. L., Kang, S. S., Lu, C. & Choi, Y. J. Quantification of YA from oyster hydrolysate for quality control and efficacy evaluation. *BioMed. Res. Int.* **2018**, 8437379 (2018).
11. Hwang, D. et al. Anti-inflammatory activity of β-thymosin peptide derived from Pacific Oyster (*Crassostrea gigas*) on NO and PGE2 production by down-regulating NF-κB in LPS-induced RAW264.7 macrophage cells. *Mar. Drugs* **17**, 129 (2019).
12. Seo, J. K. et al. Antimicrobial effect of the 60S ribosomal protein L29 (cgRPL29), purified from the gill of Pacific oyster, *Crassostrea gigas*. *Fish. Shellfish Immun.* **67**, 675–683 (2017).
13. Wang, Y. K. et al. Oyster (*Crassostrea gigas*) hydrolysates produced on a plant scale have antitumor activity and immunostimulating effects in BALB/c mice. *Mar. Drugs* **8**, 255–268 (2010).
14. Alugoju, P., Jestadi, D. & Periyasamy, L. Free radicals: properties, sources, targets, and their implication in various diseases. *Indian J. Clin. Bioche.* **30**, 11–26 (2014).
15. Umayaparvathi, S. et al. Antioxidant activity and anticancer effect of bioactive peptide from enzymatic hydrolysate of oyster (*Saccostrea cucullata*). *Biomed. Pre. Nutr.* **4**, 343–353 (2014).
16. Tanaka, K. et al. Effects of dietary oyster extract on lipid metabolism, blood pressure, and blood glucose in SD rats, hypertensive rats, and diabetic rats. *Biosci. Biotech. Bioch.* **70**, 462–470 (2006).
17. Liu, P. et al. Purification, characterization and evaluation of inhibitory mechanism of ACE inhibitory peptides from pearl oyster (*Pinctada fucata* martensii) meat protein hydrolysate. *Mar. Drugs* **17**, 463 (2019).
18. Guo, Z. et al. Heat treatments of peptides from oyster (*Crassostrea gigas*) and the impact on their digestibility and angiotensin I converting enzyme inhibitory activity. *Food Sci. Biotechnol.* **29**, 961–967 (2020).
19. Hao, L., Wang, X., Cao, Y., Xu, J. & Xue, C. A comprehensive review of oyster peptides: Preparation, characterisation and bioactivities. *Rev. Aquacult.* **14**, 120–138 (2022).
20. Xing, R. et al. Comparison of antifungal activities of scallop shell, oyster shell and their pyrolyzed products. *Egypt. J. Aquat. Res.* **39**, 83–90 (2013).
21. Upadhyay, A., Thiyagarajan, V. & Tong, Y. Proteomic characterization of oyster shell organic matrix proteins (OMP). *Bioinformation* **12**, 266–278 (2016).
22. Marin, F., Roy, N. L. & Marie, B. The formation and mineralization of mollusk shell. *Front. Mol. Biosci.* **4**, 1099–1125 (2012).

23. Feng, X. et al. Shell water-soluble matrix protein from oyster shells promoted proliferation, differentiation and mineralization of osteoblasts in *vitro* and *vivo*. *Int. J. Biol. Macromol.* **201**, 288–297 (2022).
24. Feng, X. et al. Extraction and characterization of matrix protein from Pacific oyster (*Crassostrea gigs*) shell and its anti-osteoporosis properties in vitro and in vivo. *Food Funct.* **12**, 9066–9076 (2021).
25. Lee, S. Y., Kim, H. J. & Han, J. S. Anti-inflammatory effect of oyster shell extract in LPS-stimulated Raw 264.7 cells. *Prev. Nutr. Food Sci.* **18**, 23–29 (2013).
26. Latire, T. et al. Shell extracts of the edible mussel and oyster induce an enhancement of the catabolic pathway of human skin fibroblasts, in vitro. *Cytotechnology* **69**, 815–829 (2017).
27. Ahmed, R. Evaluation of antimicrobial activity of allyl isothiocyanate (AITC) adsorbed in oyster shell on food-borne bacteria. *Clean. Technol.* **21**, 241–247 (2015).
28. Nam, B. H. et al. Functional analysis of Pacific oyster (*Crassostrea gigas*) β-thymosin: Focus on antimicrobial activity. *Fish. Shellfish Immun.* **45**, 167–174 (2015).
29. Oikawa, K. et al. Antibacterial activity of calcined shell calcium prepared from wild surf clam. *J. Health Sci.* **46**, 98–103 (2000).
30. Kim, Y. S., Choi, Y. M., Noh, D. O., Cho, S. Y. & Suh, H. J. The effect of oyster shell powder on the extension of the shelf life of tofu. *Food Chem.* **103**, 155–160 (2007).
31. Chaturvedi, R., Singha, P. K. & Dey, S. Water soluble bioactives of nacre mediate antioxidant activity and osteoblast differentiation. *Plos One* **8**, e84584 (2013).
32. Green, D. W., Kwon, H. J. & Jung, H. S. Osteogenic potency of nacre on human mesenchymal stem cells. *Mol. Cells* **38**, 267–272 (2015).
33. Shono, M. et al. Reducing effect of feeding powdered nacre of Pinctada maxima on the visceral fat of rats. *Biosci. Biotech. Bioch.* **72**, 2761–2763 (2008).
34. Chen, Y., Lin, C., Li, C. & Hwang, D. Structural transformation of oyster, hard clam, and sea urchin shells after calcination and their antibacterial activity against foodborne microorganisms. *Fish. Sci.* **81**, 787–794 (2015).
35. Sadeghi, K., Park, K. & Seo, J. Oyster shell disposal: potential as a novel ecofriendly antimicrobial agent for packaging: a mini review. *Korean J. Packag. Sci. Technol.* **25**, 57–62 (2019).
36. Huh, J. H. et al. The use of oyster shell powders for water quality improvement of lakes by algal blooms removal. *J. Korean Ceram. Soc.* **53**, 1–6 (2016).
37. Huang, X. et al. Removal of antibiotics and resistance genes from swine wastewater using vertical flow constructed wetlands: effect of hydraulic flow direction and substrate type. *Chem. Eng. J.* **308**, 692–699 (2017).
38. Khirul, M. A., Kim, B. G., Cho, D., Yoo, G. & Kwon, S. H. Effect of oyster shell powder on nitrogen releases from contaminated marine sediment. *Environ. Eng. Res.* **25**, 230–237 (2019).
39. Du, Y., Lian, F. & Zhu, L. Biosorption of divalent Pb, Cd and Zn on aragonite and calcite mollusk shells. *Environ. Pollut.* **159**, 1763–1768 (2011).
40. Moon, D. H. et al. Amelioration of acidic soil using various renewable waste resources. *Environ. Sci. Pollut. R.* **21**, 774–780 (2014).
41. Awad, Y. M., Lee, S. S., Kim, K. H., Ok, Y. S. & Kuzyakov, Y. Carbon and nitrogen mineralization and enzyme activities in soil aggregate-size classes: Effects of biochar, oyster shells, and polymers. *Chemosphere* **198**, 40–48 (2018).
42. Yao, Z. et al. Surface free energy and mechanical performance of LDPE/CBF composites containing toxic-metal free filler. *Int. J. Adhes. Adhes.* **77**, 58–62 (2017).
43. Morris, J. P., Backeljau, T. & Chapelle, G. Shells from aquaculture: a valuable biomaterial, not a nuisance waste product. *Revi. Aquacult.* **11**, 42–57 (2019).
44. Morris, J. P., Wang, Y., Backeljau, T. & Chapelle, G. Biomimetic and bio-inspired uses of mollusc shells. *Mar. Genom.* **27**, 85–90 (2016).
45. Yao, Z. et al. Bivalve shell: not an abundant useless waste but a functional and versatile biomaterial. *Crit. Rev. Environ. Sci. Tec.* **44**, 2502–2530 (2014).
46. Ovadia, Y. S. et al. Elevated serum thyroglobulin and low iodine intake are associated with nontoxic nodular goiter among adults living near the Eastern Mediterranean Coast. *J. Thyroid Res.* **2014**, 913672 (2014).
47. Jonklaas, J. et al. Guidelines for the treatment of hypothyroidism: prepared by the American Thyroid Association Task Force on thyroid hormone replacement. *Thyroid* **24**, 1670 (2014).
48. Yildirim Simsir, I., Cetinkalp, S. & Kabalak, T. Review of factors contributing to nodular goiter and thyroid carcinoma. *Med. Prin. Pract.* **29**, 1–5 (2020).
49. Li, Y., Shan, Z. & Teng, W. Effect of the transition from more than adequate iodine to adequate iodine on national changes in the prevalence of thyroid disorders: repeat national cross-sectional surveys in China. *Eur. J. Endocrinol.* **186**, 115–122 (2021).
50. Casella, C. et al. Thyroid cancer and nodules in Graves' disease: a single center experience. *Endocr. Metab. Immune Disorder.* **21**, 2028–2034 (2020).
51. Xu, J. H., Cai, P. Q., Zhou, Z. D., Qin, J. & Lin, X. P. A rare case of a postoperative submandibular exophytic goiter in a patient with a recurrent normotopic nodular goiter. *Clin. Nucl. Med.* **41**, 485–487 (2016).
52. Medeiros Neto, G., Camargo, R. Y. & Tomimori, E. K. Approach to and treatment of goiters. *Med. Clin. N. Am.* **96**, 351–368 (2012).
53. Shi, H. et al. Risk factors for the relapse of Graves' disease treated with antithyroid drugs: a systematic review and meta-analysis. *Clin. Ther.* **42**, 662–675 (2020).
54. Yang, M. L. & Lu, B. Treatment of goiter with traditional Chinese medicine regimen Xing Qi Hua Ying Tang: a clinical study on 72 patients with multinodular and diffuse goiter. *J. Altern. Complement. Med.* **24**, 374–377 (2018).
55. Peng, Q., Hong, Y. & Liao, G. Experimental study of six testacean TCM 'endometriosis' role on goiter model rats. *J. Zhejiang Chi. Med. Univ.* **37**, 1429–1432 (2013).
56. Li, M. et al. Exploring the effect and mechanism of Haizao Yuhu decoction containing three variants of glycyrrhiza on goiter using an integrated strategy of network pharmacology and RNA sequencing. *J. Ethnopharmacol.* **316**, 116750 (2023).
57. Dong, S. et al. Xiao-Luo-Wan treats propylthiouracil-induced goiter with hypothyroidism in rats through the PI3K-AKT/RAS pathways based on UPLC/MS and network pharmacology. *J. Ethnopharmacol.* **289**, 115045 (2022).
58. Li, N. et al. Haizao Yuhu decoctions including three species of glycyrrhiza protected against propylthiouracil-induced goiter with hypothyroidism in rats via the AMPK/mTOR pathway. *J. Ethnopharmacol.* **296**, 115443 (2022).
59. Tian, G. et al. The evolution of small-molecule Akt inhibitors from hit to clinical candidate. *Eur. J. Med. Chem.* **279**, 116906 (2024).
60. Hassan, D., Menges, C. W., Testa, J. R. & Bellacosa, A. AKT kinases as therapeutic targets. *J. Exp. Clin. Can. Res.* **43**, 313 (2024).
61. Liu, T. et al. Advances of phytotherapy in ischemic stroke targeting PI3K/Akt signaling. *Phytother. Res.* **37**, 5509–5528 (2023).
62. Kong, J. et al. Nephrotoxicity assessment of podophyllotoxin-induced rats by regulating PI3K/Akt/mTOR-Nrf2/HO1 pathway in view of toxicological evidence chain (TEC) concept. *Ecotoxicol. Environ. Saf.* **264**, 115392 (2023).
63. Khezri, M. R., Hsueh, H., Mohammadipanah, S., Fard, J. K. & Berenji, M. G. The interplay between the PI3K/AKT pathway and circadian clock in physiologic and cancer-related pathologic conditions. *Cell Prolif.* **57**, e13608 (2024).

64. Selvakumar, S. C., Preethi, K. A. & Sekar, D. MicroRNAs as important players in regulating cancer through PTEN/PI3K/AKT signalling pathways. *BBA Rev. Cancer* **3**, 188904 (2023).
65. Tian, M. & Qi, Z. Study on the mechanism of Liqi Xiaoying Recipe on rats with nodular goiter based on PI3K/Akt signal pathway. *China Pract. Med.* **16**, 206–208 (2021).
66. Liang, W., Sun, Y., Chen, L., Cheng, W. & Li, W. Intervention mechanism of Xiaoluowan on experimental goiter rats based on PI3K/Akt/mTORC1 pathway. *Chin. J. Exp. Tradit. Med. Form.* **28**, 30–36 (2022).

Acknowledgements

This study was funded by the Xinglin Scholar Discipline Promotion Talent Program of Chengdu University of Traditional Chinese Medicine [QJJJ2024014] and the National Administration of Traditional Chinese Medicine [gzyjc20210901]. The funder played no role in study design, data collection, analysis and interpretation of data, or the writing of this manuscript.

Author contributions

Hongyi Zhang: Data curation, Formal analysis, Investigation, Methodology, Software, Visualization, Writing-original draft. Qiaoling Ma: Data curation, Investigation, Software, Visualization. Weichao Wang: Data curation, Methodology, Software, Visualization. Bin Wang: Data curation, Formal analysis, Methodology. Jiawen Liu: Data curation, Investigation, Software. Fu Wang: Investigation, Methodology. Yuan Hu: Conceptualization, Data curation. Lin Chen: Funding acquisition, Software, Validation. Youping Liu: Conceptualization, Methodology, Project administration, Supervision. Qi Wang: Conceptualization, Supervision, Validation. Hongping Chen: Resources, Supervision, Validation, Writing-review and editing.

Competing interests

The authors declare no competing interests.

Additional information

Supplementary information The online version contains supplementary material available at https://doi.org/10.1038/s41538-025-00483-y.

Correspondence and requests for materials should be addressed to Qi Wang or Hongping Chen.